ORGANOMETALLICS

Article

pubs.acs.org/Organometallics

Iron and Ruthenium Heterobimetallic Carbonyl Complexes as Electrocatalysts for Alcohol Oxidation: Electrochemical and Mechanistic Studies

Daniel Serra, Marie C. Correia, and Lisa McElwee-White*

Department of Chemistry and Center for Catalysis, University of Florida, Gainesville, Florida 32611-7200, United States

Supporting Information

ABSTRACT: Carbonyl-containing Ru and Fe heterobimetallic complexes were prepared and tested as electrocatalysts for the oxidation of methanol and ethanol. GC analysis of the electrolyte solution during bulk electrolysis indicated that CpRu(CO)(μ-I)(μ-dppm)PtI_2 (**1**), CpFe(CO)(μ-I)(μ-dppm)-PtI_2 (**2**), and CpRu(CO)(μ-I)(μ-dppm)PdI_2 (**3**) were catalysts for the electrooxidation of methanol and ethanol, while CpFe(CO)(μ-I)(μ-dppm)-PdI_2 (**4**), CpRu(CO)I(μ-dppm)AuI (**5**), and CpFe(CO)I(μ-dppm)AuI (**6**) did not function as catalysts. The oxidation of methanol resulted in two- and four-electron oxidation to formaldehyde and formic acid, respectively, followed by condensation with unreacted methanol to yield dimethoxymethane and methyl formate as the observed products. The oxidation of ethanol afforded 1,1′-diethoxyethane as a result of two-electron oxidation to acetaldehyde and condensation with excess ethanol. FTIR analysis of the headspace gases during the electrochemical oxidation of methanol indicated formation of CO_2. Isotopic labeling experiments demonstrated that the CO_2 resulted from oxidation of the CO ligand instead of complete oxidation of CH_3OH.

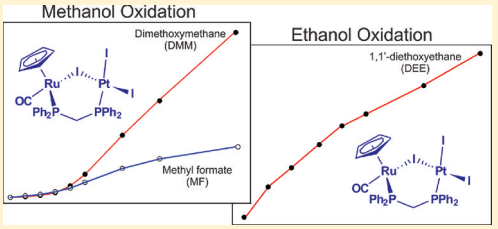

INTRODUCTION

Heterobinuclear complexes have long been investigated as catalysts, due to the potential for reactivity different from that of their mononuclear analogues.[1−11] In such species, the two metals can work cooperatively or each can perform a different task which leads to an overall increase in activity.[12−23]

Such an effect has been noted for the electrooxidation of methanol using various electrode materials: initially Pt anodes[24−30] and then more complex alloys[31−40] and nanoparticles.[41−45] Surface studies on Pt anodes showed that Pt is poisoned by adsorbed CO, which is formed as an intermediate during the electrooxidation process.[30,46−49] Combining Pt with a second metal improved the anode behavior, and systems utilizing the bimetallic RuPt anode proved to be particularly effective.[50−55] This effect has been attributed to the "bifunctional mechanism" initially proposed by Watanabe and Motoo, in which Pt sites are responsible for the binding and dehydrogenation of methanol while Ru sites activate water through formation of Ru−oxo intermediates, which are then involved in conversion of surface-bound CO to CO_2.[54−58]

Previous studies of the electrochemical oxidation of methanol using the heterobimetallic catalysts Cp(PPh_3)Ru(μ-Cl)(μ-dppm)$PtCl_2$ (**7**; dppm = bis(diphenylphosphino)-methane),[59] Cp(PPh_3)Ru(μ-Cl)(μ-dppm)$PdCl_2$ (**8**),[60] and Cp(PPh_3)RuCl(μ-dppm)AuCl (**9**)[60] were consistent with a beneficial effect of the second metal, since an enhancement of the catalytic activity was observed in comparison to that for the monomeric model compounds CpRu(κ^2-dppm)Cl[61] and Cp$Ru(PPh_3)_2$Cl.[62]

In the past decade catalysis with iron complexes has attracted significant attention, due to their low price and ready availability.[63−69] Recently, we reported the synthesis and characterization of carbonyl-containing Ru/Pt, Ru/Pd, and Ru/Au complexes as well as their isoelectronic Fe/Pt, Fe/Pd, and Fe/Au analogues.[70] These complexes allow us not only to compare the reactivity of iron with ruthenium but also to probe whether bound CO could be oxidized under electrochemical conditions if it is generated as an intermediate. As a continuation of our work, we now report investigations on electrocatalytic oxidation of methanol and ethanol using these compounds as well as isotopic labeling studies in which ^{13}C-labeled ^{13}C-Ru/Pt and ^{13}C-Fe/Pt complexes are used to probe the source of CO_2 observed upon electrooxidation of methanol.

EXPERIMENTAL SECTION

General Procedures. All reactions and manipulations were performed under an argon atmosphere using standard Schlenk techniques. Pentane and diethyl ether were dried by distillation from Na/Ph_2CO. Acetonitrile and 1,2-dichloroethane (DCE) were dried by distillation from CaH_2. Methanol and ethanol were dried by distillation from magnesium. Benzene and dichloromethane were dried using an MBraun solvent purification system. All solvents were saturated with argon prior to use. All deuterated solvents for NMR measurements were degassed via freeze−pump−thaw cycles and stored over activated molecular sieves (4 Å). ^{1}H, ^{13}C, and ^{31}P NMR spectra were recorded at room temperature on a Varian Mercury 300 spectrometer operating at 300, 75, and 121 MHz, respectively. Chemical shifts (δ, ppm) are

Received: November 14, 2010
Published: October 24, 2011

reported relative to either residual solvent peaks (^{1}H, ^{13}C NMR) or 85% H_3PO_4 (^{31}P NMR). IR spectra were obtained as neat films on NaCl using a a Perkin-Elmer Spectrum One FTIR spectrophotometer. $CpRu(CO)_2I$ (**11**),[71] $CpRu(CO)(PPh_3)I$ (**14**),[72] $CpRu(CO)(\kappa^1$-dppm)I, $[CpRu(CO)(\kappa^2$-dppm)]I,[70,73] $CpRu(CO)(\mu$-I)(μ-dppm)PtI_2 (**1**),[70] $CpRu(CO)(\mu$-I)(μ-dppm)PdI_2 (**3**), $CpRu(CO)I(\mu$-dppm)AuI (**5**), $CpFe(CO)_2I$ (**13**),[71] $CpFe(CO)(PPh_3)I$ (**15**),[74] $CpFe(CO)(\kappa^1$-dppm)I,[75] $CpFe(CO)(\mu$-I)(μ-dppm)PtI_2 (**2**),[70] $CpFe(CO)(\mu$-I)(μ-dppm)PdI_2 (**4**), $CpFe(CO)I(\mu$-dppm)AuI (**6**), and $CpRu(\eta^3$-allyl)Cl_2 (**10**)[76] were prepared as previously described. CpFe(benzene)PF_6 and all other starting materials were purchased in reagent grade purity and used without further purification.

Electrochemical experiments were performed at ambient temperature in a glovebox using an EG&G PAR Model 263A potentiostat/galvanostat. Cyclic voltammograms (CV) were performed in a three-compartment H-cell separated by a medium-porosity sintered-glass frit using either 0.1 M tetrabutylammonium trifluoromethanesulfonate (TBAT) or 0.1 M tetrabutylammonium hexafluorophosphate (TBAH) dissolved in 3.5 mL of DCE and a 5 mM catalyst concentration. All potentials are reported vs NHE and referenced to Ag/Ag^+. The reference electrode consisted of a silver wire immersed in an acetonitrile solution containing freshly prepared 0.01 M $AgNO_3$ and 0.1 M TBAT or TBAH. The Ag^+ solution and silver wire were contained in a 75 mm glass tube fitted at the bottom with a Vycor tip. A highly polished glassy-carbon electrode (3 mm diameter) was the working electrode, and a platinum flag was used as the counter electrode. Bulk electrolysis was performed using a reticulated vitreous carbon working electrode instead of the glassy-carbon electrode and 0.1 M tetrabutylammonium tetrafluoroborate ($TBABF_4$) dissolved in either MeOH or EtOH as the electrolytic solution. The $E°$ values for the ferrocenium/ferrocene couple in DCE, MeOH, and EtOH were +0.72, +0.62, and +0.68 V vs NHE, respectively.[59−62,70]

Typical bulk electrolysis experiments were performed using complex concentrations of 10 mM in 3.5 mL electrolytic solution and allowing the reaction to proceed until 200 C of charge was passed into the system (about 24 h). Experiments were also extended for an additional 24 h with some systems to test the degradation behavior of the complexes over longer time periods (presented in the Supporting Information). Analyses of the oxidation products from bulk electrolyses were performed using gas chromatography on a Shimadzu GC-17A chromatograph. In the case of methanol, a 15 m × 0.32 mm column of AT-WAX (Alltech, 0.5 μm film) on fused silica was utilized while a 15 m × 0.53 mm DB-5 fused silica column (J & W Scientific, 1.5 μm film) was used to analyze the oxidation products of ethanol. The columns were attached to the injection port with a neutral 5 m × 0.32 mm deactivated guard column. Quantitative analysis utilized a known amount of *n*-heptane or *n*-octane as an internal standard, and identification was confirmed by comparison of the retention times of the oxidation products with those of authentic samples. In addition to liquid samples, headspace gas samples were removed from the cell using a gastight syringe and analyzed in a gas cell by FTIR.

$CpRu(^{13}CO)_2Cl$ (11-^{13}CO). In a high-pressure vessel, a suspension of complex **10** (0.15 g, 0.54 mmol) in 3 mL of decane was stirred for 2 h under 1 atm of ^{13}CO at 140 °C. The cooled solution was passed through a silica gel column with hexane as eluent to remove the decane solvent; then elution with ether afforded pure **11-^{13}CO**. Yield: 0.11 g, 76%. ^{1}H NMR ($CDCl_3$): δ 5.44 (s, 5H, (C_6H_5)). ^{13}C NMR ($CDCl_3$): δ 196.0, 87.7. ν_{CO}: 1998, 1918 cm^{-1}. The compound was identified by comparison to literature data for unlabeled **11**.[77,78]

$[CpFe(^{13}CO)_2]_2$ (12-^{13}CO). A solution of CpFe(benzene)PF_6 (0.65 g, 2.3 mmol) in 10 mL of THF was stirred with 15 g of sodium amalgam (1%) at −20 °C. After 1 h, the resulting dark green solution was transferred via cannula to another Schlenk flask and the solvent was evaporated under vacuum. The resulting residue was then extracted with cold pentane and the filtrate dried under vacuum. The crude CpFe(benzene) was dissolved in cold THF (40 mL), added to a 300 mL Parr pressure vessel with a glass liner at −78 °C, and stirred at ambient temperature under 1 atm of ^{13}CO for 24 h. After evaporation of the THF, extraction with toluene (2 × 30 mL), and removal of toluene under vacuum, a dark red solid was obtained. Yield: 0.31 g, 77%. ^{1}H NMR (C_6D_6): δ 4.10 (s, 5H, (C_6H_5)). ν_{CO}: 1943, 1900, 1815, 1733 cm^{-1}. The compound was identified by comparison to literature data on unlabeled **12**.[79]

CpFe(^{13}CO)$_2$I (13-^{13}CO). A solution of **12-^{13}CO** (0.31 g, 0.87 mmol) and I_2 (0.44 g, 1.2 mmol) in chloroform (30 mL) was refluxed for 1 h. After it was cooled to room temperature, the organic solution was washed with an aqueous solution of sodium thiosulfate (5 g in 150 mL). Evaporation of the solvent followed by washing with pentane resulted in a dark brown solid. Yield: 0.29 g, 55%. ^{1}H NMR ($CDCl_3$): δ 4.97 (s, 5H, (C_6H_5)). ^{13}C NMR ($CDCl_3$): δ 213.2, 84.9. ν_{CO}: 1986, 1941 cm^{-1}. The compound was identified by comparison to literature data on unlabeled **13**.[80]

RESULTS AND DISCUSSION

Synthesis of Heterobimetallic Complexes 1−6. Preparation and spectroscopic data for complexes **1−6** have been reported previously.[70]

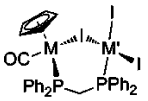

Complex	M	M'
1	Ru	Pt
2	Fe	Pt
3	Ru	Pd
4	Fe	Pd

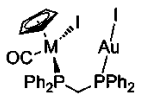

Complex	M
5	Ru
6	Fe

Synthesis of the ^{13}C-Labeled Ru/Pt Complex 1-^{13}CO. The Ru/Pt complex **1-^{13}CO** was synthesized by starting from $CpRu(PPh_3)_2Cl$ using a literature procedure.[76] Incorporation of the labeled carbonyl was achieved via oxidative addition of allyl chloride to $CpRu(PPh_3)_2Cl$ (45% yield) to afford the Ru(η^3-allyl) complex **10**, followed by reductive elimination in the presence of ^{13}CO to produce the labeled complex **11-^{13}CO** in 80% yield (Scheme 1). Subsequent steps to the Ru/Pt

Scheme 1. Synthesis of the Labeled Complex 1-^{13}CO

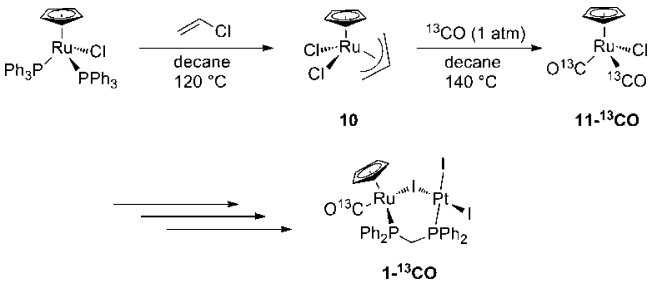

heterobimetallic complex **1-^{13}CO** have been described previously for the unlabeled compound[70] and will not be discussed further. CO stretching frequencies for the labeled compounds were determined by comparison to the reported values for the unlabeled compounds and are provided in Supporting Information (Table S1).[70]

Synthesis of the ^{13}C-Labeled Fe/Pt Complex 2-^{13}CO. Preparation of the ^{13}CO-Fe/Pt complex **2-^{13}CO** followed a pathway different from that used for the Ru/Pt complex **1-^{13}CO**, due to difficulties in isolating CpFe(η^3-allyl)Cl_2. In order to incorporate the carbonyl ligands, the commercially available CpFe(benzene)PF_6 was chosen as starting material. Reduction of this compound by Na/Hg leads to CpFe(benzene), which undergoes facile substitution of the benzene ligand by ^{13}CO to yield the labeled $[CpFe(^{13}CO)_2]_2$ dimer **12-^{13}CO**. Further reaction with iodine in refluxing chloroform

dx.doi.org/10.1021/om101070z | Organometallics 2011, 30, 5568−5577

led to the formation of $CpFe(^{13}CO)_2I$ (**13-^{13}CO**) (Scheme 2). Again, the subsequent steps to compound **2-^{13}CO** have been

Scheme 2. Synthesis of the Labeled Complex 2-^{13}CO

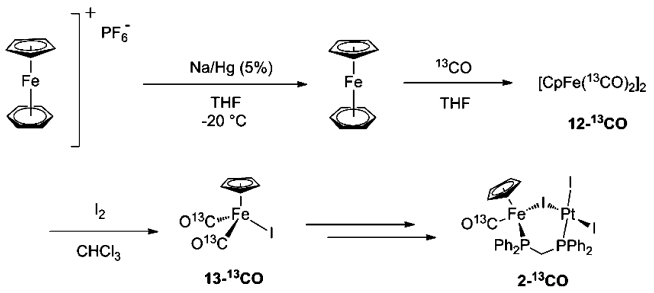

described previously for the unlabeled compound[70] and will not be discussed here. IR stretching frequencies for the labeled compounds were determined by comparison to the reported values for the unlabeled compounds and are available in the Supporting Information (Table S1).[70,81,82]

Electrochemical Oxidation of Methanol with Heterobimetallic Complexes 1–6. As previously described,[59,60,83] cyclic voltammetry in the presence of methanol is a convenient way to screen for catalytic activity toward methanol electrooxidation. The cyclic voltammograms of the Ru/Pt complex **1** (Figure 1), Ru/Pd complex **3**, and Fe/Pd complex **4**

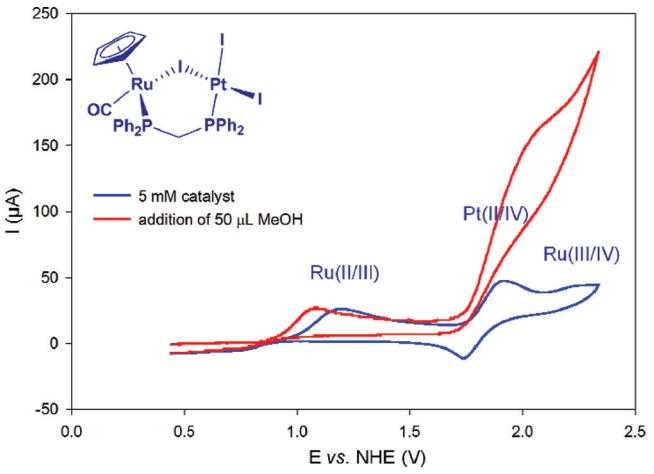

Figure 1. Cyclic voltammograms of complex **1**. Conditions: 0.1 M TBAH/DCE; 50 mV s^{-1} scan rate; glassy-carbon working electrode; Ag/Ag^+ reference electrode.

(Supporting Information, Figures S1 and S2), all show significant increases in current after addition of 50 μL of methanol to the system. These current increases usually coincide with the redox potential of the second metal and are an indication of a catalytic process for methanol oxidation. In contrast to complexes **1**, **3**, and **4**, the cyclic voltammogram for the isoelectronic Fe/Pt complex **2** (Figure 2) exhibits small increases in current at the Fe(II/III), Pt(II/IV), and Fe(III/IV) redox waves after addition of methanol, suggesting minimal reactivity toward methanol. The Ru/Au complex **5** was found to be the least stable of all the complexes, with decomposition of the solid compound occurring after several weeks in the drybox and evidence of the decomposition being observed during cyclic voltammetry. The cyclic voltammogram of complex **5** could be obtained; however, rapid dissociation of

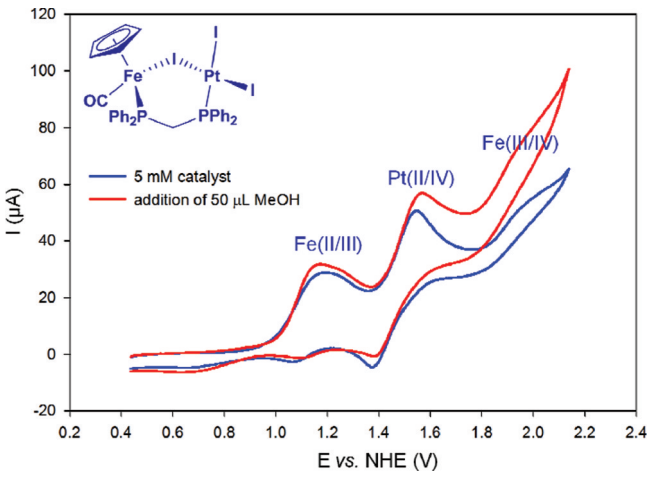

Figure 2. Cyclic voltammograms of complex **2**. Conditions: 0.1 M TBAT/DCE; 50 mV s^{-1} scan rate; glassy-carbon working electrode; Ag/Ag^+ reference electrode.

the heterobimetallic structure to the fragment $[CpRu(CO)(\kappa^2\text{-dppm})]I$ was observed after several cycles (Figures S3a and S3b, Supporting Information).

At the beginning of the CV, there is an irreversible Ru(II/III) redox wave, which rapidly becomes reversible with a slight shift to lower potential as **5** is converted to $[CpRu(CO)(\kappa^2\text{-dppm})]I$. This observation was confirmed by comparison with independently prepared $[CpRu(CO)(\kappa^2\text{-dppm})]I$. The dppm-bridged Fe/Au complex **6** was slightly more stable under cyclic voltammetry conditions and exhibited three oxidation waves, which were assigned to Fe(II/III), Au(I/III), and Fe(III/IV) couples, respectively (Figure 3).

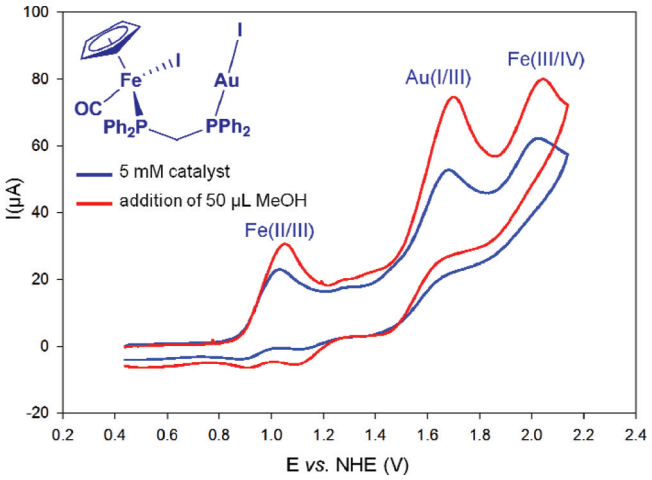

Figure 3. Cyclic voltammograms of complex **6**. Conditions: 0.1 M TBAT/DCE; 50 mV s^{-1} scan rate; glassy-carbon working electrode; Ag/Ag^+ reference electrode.

After addition of methanol, increases in the oxidative current were observed for the Ru/Au complex **5** as well as for the Fe/Au complex **6**. For **5**, these increases coincide with the Au(I/III) couple and the Ru(III/IV) redox waves, while for **6**, increases are observed for the Fe(II/III), Au(I/III), and Fe(II/IV) redox waves, which suggest reactivity toward methanol. Since the products of methanol oxidation were not detected during bulk electrolyses involving **5** and **6**, it is possible that these increases in current are the result of stoichiometric

dx.doi.org/10.1021/om101070z | Organometallics 2011, 30, 5568–5577

reactions with methanol. This process was also previously observed for the analogous PPh_3 complex $CpRu(PPh_3)I(\mu$-dppm)AuI.[61]

In order to assess the catalytic behavior of complexes **1**–**6**, bulk electrolysis of methanol was carried out for product identification and quantification. The initial electrooxidation experiments using complexes **1**–**6** were performed in 0.7 M TBAT/DCE at a potential of 1.7 V vs NHE, as carried out in previous studies.[60,61] Under these conditions, poor results were obtained, due to degradation of the catalysts and/or side reactions with the chlorinated solvent resulting in inhibition of catalysis.

Surprisingly, neat methanol proved to be a viable solvent, since the carbonyl compounds **1**–**6** are more soluble in methanol than the analogous triphenylphosphine complexes.[59−61,84] Experiments in neat methanol afforded an improvement in the current efficiencies and turnover numbers as compared to those performed in the nonpolar solvent DCE. Due to the more limited anodic range of methanol, bulk electrolysis in methanol was performed at 1.5 V vs NHE in 0.1 M $TBABF_4$, as previously described for the related amino-substituted cyclopentadienyl complexes.[85] At 1.5 V vs. NHE, control experiments showed no evidence of methanol oxidation products in the absence of catalyst. An additional control experiment was performed by recycling a used reticulated vitreous carbon electrode to test for heterogeneous electrocatalysis by material deposited on the electrode surface during the reaction. The bulk electrolysis of methanol was performed using Ru/Pt catalyst **1**; at the end of this reaction, the working electrode was removed, rinsed gently with water and then methanol, and left to air-dry overnight. This used electrode was then placed in a cell containing fresh 0.1 M $TBABF_4$/MeOH solution and charge passed for a time corresponding to the bulk electrolysis experiments. During this time, no methanol oxidation products were observed upon GC analysis of liquid samples.

The products observed during electrooxidation of methanol in the presence of complexes **1**–**3** are those detected in previous studies:[60,61,85] dimethoxymethane (DMM) and methyl formate (MF). These products arise from condensation of the primary oxidation products, formaldehyde and formic acid, with methanol. Carbon dioxide (CO_2) formation was also detected by FTIR analysis of the headspace gases during the electrooxidation of methanol using heterobimetallic complexes **1** and **2** (vide infra). The product ratios, current efficiencies (CE), and numbers of turnovers (TO) for the electrochemical oxidation of methanol by catalysts **1**–**4** are summarized in Table 1. Results for the mononuclear model compounds $CpRu(CO)_2I$ (**11**), $CpFe(CO)_2I$ (**13**), $CpRu(CO)(PPh_3)I$ (**14**), $CpFe(CO)(PPh_3)I$ (**15**), $[CpRu(\kappa^2$-dppm)(CO)]I, and $Pt(COD)I_2$ as well as those from the combination of complex **14** or **15** with $Pt(COD)I_2$ are presented in Table 2. $Pd(COD)I_2$ could not be used as a model compound, because attempts to synthesize it led to undefined mixtures, due to the low stability of the compound.

Attempts to perform bulk electrolyses with the heterobimetallic Ru/Au and Fe/Au complexes **5** and **6** proved to be very difficult, due to poor stability of the complexes during electrolysis. In fact, small traces of the two- and four-electron-oxidation products DMM and MF were detected in the case of complex **5** but rapid degradation was also observed, as the solution changed from pale yellow to colorless after about 50 C of charge was passed. No additional charge could be passed after the color change was observed. Attempts to identify degradation products from the residual solid (after removal of the solvent) by ^{31}P NMR or FTIR spectroscopy were unsuccessful, due to the high electrolyte concentration present in the residue. The same decoloration could be observed upon electrolysis of the Fe/Au complex **6** in methanol; however, no traces of DMM or MF were detected by GC or FTIR analysis. These results indicate that stoichiometric reactions may presumably be involved between complexes **5** and **6** in the presence of methanol rather than catalytic oxidation of methanol, which could be responsible for the current enhancements observed during the cyclic voltammetry experiments after addition of methanol. Complexes **5** and **6** were not investigated further, due to their rapid degradation under the experimental conditions.

Table 1. Bulk Electrolysis Data for the Oxidation of Methanol by Complexes 1−4 under Dry Conditions and in the Presence of Water[f]

	product ratio (DMM/MF)[a,b]					
	Ru/Pt (**1**)		Fe/Pt (**2**)		Ru/Pd (**3**)	
charge (C)	dry	wet[c]	dry	wet[c]	dry	wet[c]
20	0.4	0	n/o	n/o	0.2	0
40	0.6	0.6	n/o	n/o	0.4	0.1
60	0.8	1.2	n/o	∞	0.5	0.3
80	1.2	1.6	∞	∞	0.7	0.5
100	1.5	1.9	∞	∞	0.8	0.6
150	2.1	2.7	∞	2.0	1.1	1.1
200	2.5	3.5	∞	2.2	1.1	1.5
	Ru/Pt (**1**)		Fe/Pt (**2**)		Ru/Pd (**3**)	
	dry	wet[c]	dry	wet[c]	dry	wet[c]
CE[d] (%) after 200 C	63.1	47.9	4.9	8.6	22.8	12.6
TO[e] after 200 C	12	10	1	1	4	2

[a]Electrolyses were performed at 1.5 V vs NHE in pure methanol. A 10 mM catalyst concentration was used for each experiment. [b]Determined by GC with respect to *n*-heptane as an internal standard. n/o = no observable product. [c]Addition of 10 μL of water before electrolysis. [d]CE denotes the ratio of charge needed to produce the observed yields of DMM and MF vs the total charge passed during the experiment. [e]TO denotes the number of moles of DMM and MF produced per mole of catalyst. [f]Catalysis with the Fe/Pd complex **4** showed no product formation.

Generally, the ruthenium-containing heterobimetallic complexes were found to have superior activity compared to their iron congeners. Typically, no (complexes **4** and **6**) or poor (complex **2**) activities were observed for the iron-containing compounds during electrooxidation of methanol. Although the Fe/Pt complex **2** formed the two-electron oxidation product DMM selectively, only 4.9% CE could be achieved with approximately 1 TO after 200 C of charge was passed (Figure 4, Table 1).

In methanol, the Ru/Pt complex **1** was the most active catalyst among all the carbonyl compounds, reaching 63.1% CE and 12 TO, after 200 C of charge had been passed (Figure 5, Table 1). Under these conditions, compound **1** proved to be a superior catalyst compared to the analogous complexes incorporating PPh_3 instead of the CO ligand. At low conversion, MF is present in higher concentration than DMM (ratio: 0.4 at 20 C) until about 62 C of charge is passed, then for the remainder of the experiment the two-electron-oxidation product DMM is observed in higher concentration (ratio: 2.5 at 200 C). This change in

dx.doi.org/10.1021/om101070z|*Organometallics* 2011, 30, 5568−5577

Table 2. Bulk Electrolysis Data for the Oxidation of Methanol with Mononuclear Model Complexes

	product ratio (DMM/MF)[a,b]							
charge (C)	$CpRu(CO)_2I$ (**11**)	$CpFe(CO)_2I$ (**13**)	$CpRu(CO)(PPh_3)I$ (**14**)	$CpFe(CO)(PPh_3)I$ (**15**)	$[CpRu(\kappa^2\text{-dppm})(CO)]I$	Ru (**14**) + $Pt(COD)I_2$	Fe (**15**) + $Pt(COD)I_2$	$Pt(COD)I_2$
50	n/o	n/o	0.8	n/o		∞	n/o	
100	n/o	n/o	1.1	n/o	n/o	8.6	n/o	
150						10.8		
200	∞	n/o	1.3	n/o	4.2	14.3	∞	4.4

	$CpRu(CO)_2I$ (**11**)	$CpRu(CO)(PPh_3)I$ (**14**)	$[CpRu(\kappa^2\text{-dppm})(CO)]I$	Ru (**14**) + $Pt(COD)I_2$	Fe (**15**) + $Pt(COD)I_2$	$Pt(COD)I_2$
CE[c] (%) after 200 C	0.4	21.4	0.7	27.3	0.2	5.7
TO[d] after 200 C	<1	3	<1	6	<1	1

[a]Electrolyses were performed at 1.5 V vs NHE in pure methanol. A 10 mM catalyst concentration was used for each experiment. [b]Determined by GC with respect to *n*-heptane as an internal standard. n/o = no observable product. [c]CE denotes the ratio of charge needed to produce the observed yields of DMM and MF vs the total charge passed during the experiment. [d]TO denotes the number of moles of DMM and MF produced per mole of catalyst.

chemoselectivity suggests that the active catalyst changes during the electrolysis process. The initial active species serves as a four-electron-oxidation catalyst but is then converted to a two-electron oxidant as the experiment progresses.

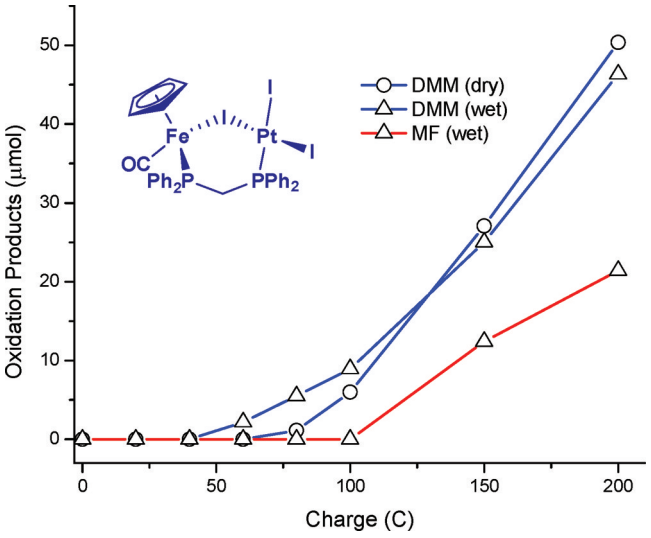

Figure 4. Product evolution for the electrooxidation of methanol using the Fe/Pt complex **2**.

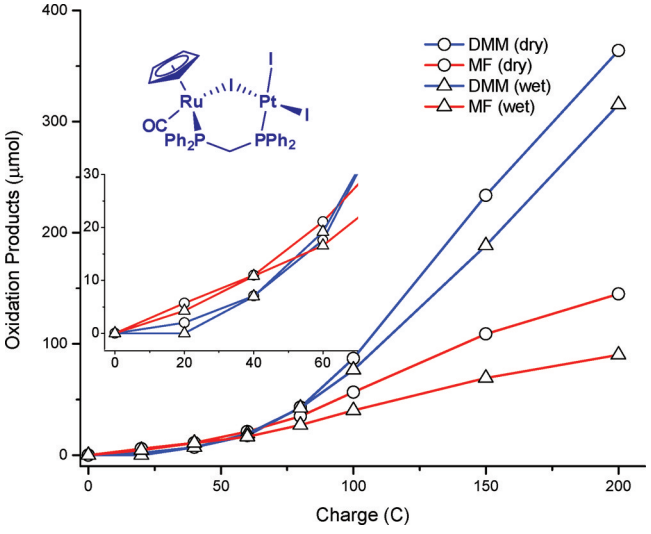

Figure 5. Product evolution for the electrooxidation of methanol using the Ru/Pt complex **1**.

The Ru/Pd carbonyl complex **3** gave lower current efficiency and number of turnovers (22.8% and 4) in comparison to the Ru/Pt complex **1**. The product ratios and product evolution for **3** (Table 1 and Supporting Information, Figure S6) also show a partitioning of the oxidation products more favorable to MF than that of **1**. At the beginning of catalysis, the four-electron-oxidation product MF is favored until about 125 C is passed, then approximately a 1:1 ratio of DMM to MF is detected until the end of the experiment. Control reactions with mononuclear model compounds were performed in order to compare their activities for the electrooxidation of methanol with those of the heterobimetallic complexes (Table 2). Neither $CpFe(CO)_2I$ (**13**) nor $CpFe(CO)(PPh_3)I$ (**15**) showed any catalytic activity for methanol oxidation. This is not surprising, since the Fe heterobimetallic complexes show poor (Fe/Pt complex **2**) or no (Fe/Pd and Fe/Au complexes **4** and **6**) activity for the process. A 1:1 mixture of complex **15** and $Pt(COD)I_2$ was also tested, since the Fe/Pt complex **2** showed some activity (4.9% CE and 1 TO). However, only traces of DMM could be detected after 200 C of charge was passed into the system. Although the results from the Fe/Pt complex **2** were poor in comparison to those for the Ru-containing heterobimetallic complexes, the beneficial effect of using heterobimetallic complexes could also be observed with **2**, since neither model compound **13** nor **15** was active.

Although several mononuclear ruthenium complexes were tested in the control reactions, only $CpRu(CO)(PPh_3)I$ (**14**) showed activity for methanol electrooxidation (21.4% CE, TO = 3 after 200 C). These results are similar to those from the Ru/Pd complex **3** (22.8% CE, TO = 4); however, they are much lower compared to those for the Ru/Pt complex **1** (63.1% CE, TO = 12, Tables 1 and 2).

Finally, a mixture of $CpRu(CO)(PPh_3)I$ (**14**) and $Pt(COD)I_2$ was also tested in a control experiment. In contrast to the case for the Fe complex **15**, when **14** was used in combination with $Pt(COD)I_2$ slightly higher activity (27.3% CE, TO = 6) was exhibited than when the mononuclear Ru complex **14** was used alone. Since $Pt(COD)I_2$ shows some activity (5.7% CE and 1 TO), the catalysis resulting from the mixture was attributed to the combined activities of complex **14** and $Pt(COD)I_2$. However, since the amount of products generated with the heterobimetallic Ru/Pt complex **1** is greater than that for the resulting combination of the two model compounds, the

dx.doi.org/10.1021/om101070z|*Organometallics* 2011, 30, 5568–5577

higher activity of **1** can be attributed to the enhancement of reactivity due to the close proximity of the two metal centers in complex **1**. This is consistent with a heterobimetallic catalyst being the active species during electrocatalytic oxidation of methanol.

As in previous studies with related complexes,[60] the electrochemical oxidation of methanol was also performed in the presence of 10 μL of water added to the system before the experiment was started. Results are presented in Table 1 for the heterobimetallic complexes **1**–**4**. For the directly related triphenylphosphine compounds,[59−61,83,78] the presence of added water at an early stage of the electrolysis (before it is generated by condensation of the primary products with methanol) favored the formation of the more oxidized product MF. In contrast, the Ru−CO complexes tended to exhibit lower activities when water was added before the experiment. The Ru/Pt and Ru/Pd complexes **1** and **3** respectively exhibited decreases in current efficiencies from 63.1% to 47.9% for **1** and from 22.8% to 12.6% for **3** (Table 1 and Supporting Information, Figure S6) under wet conditions. The presence of water seems to slightly influence the chemoselectivity for both complexes **1** and **3**; at the end of the experiments under wet conditions, they exhibited somewhat higher ratios of DMM/MF in comparison to the reactions with no added water (2.5 vs 3.5 for **1** and 1.1 vs 1.5 for **3**). Close observation of the product ratios and product evolution for **1** show that in the early stage of the catalysis under wet conditions, MF was favored until about 52 C of charge had been passed (Figure 5), and then DMM was formed preferentially until the end of the experiment; the MF-DMM selectivity switch is observed 10 C earlier in comparison to the case for dry conditions. In contrast, complex **3** exhibits similar behavior, with MF being formed as the major product until about 140 C and then DMM again becoming the favored oxidation product until the end of the experiment (200 C). This MF−DMM selectivity switch was observed later in the experiment for wet conditions (140 C) compared to the case for dry conditions (124 C). The major changes are mainly due to the activity of the Ru/Pt catalyst **1** or the Ru/Pd complex **3**, which declined in the presence of added water, presumably due to a deactivation (and/or decomposition) process. This observation is consistent with the results obtained during the FTIR experiments for complex **1** (vide infra).

Surprisingly, the Fe/Pt complex **2** showed a small increase in current efficiency under wet conditions (8.6% vs 4.9% at 200 C) and, in contrast to the Ru/M (M = Pt (**1**), Pd (**3**)) systems, also showed improvement when water was added at the beginning of the experiment. This increase in activity is mainly due to the additional formation of the four-electron product MF in comparison to the experiment performed under dry conditions (Table 1, Figure 4). Indeed, only the two-electron product DMM was observed under dry conditions, while in the presence of added water, DMM and MF were produced with a DMM:MF ratio reaching 2.2:1 after 200 C of charge was passed. Continuation of bulk electrolysis until 402 C demonstrated that the complex did not lose its activity and a maximum of 10.4% CE and TO = 4 could be reached at the end of the experiment (Supporting Information, Figure S5). In the case of the Fe/Pt complex **2**, added water is required for the formation of the four-electron-oxidation product, while in the case of the Ru/M systems **1** and **3**, deliberate addition of water seems to suppress the formation of both DMM and MF.

As also observed for dry methanol, electrolysis of the heterobimetallic Fe/Pd complex **4** in the presence of water did not result in formation of any products that could be detected in solution by GC or in the headspace by FTIR.

Electrochemical Oxidation of Ethanol with Heterobimetallic Complexes 1−6. Electrocatalytic oxidation of ethanol has been shown to yield a complicated mixture of products. Similar to methanol electrooxidation by homogeneous catalysts, oxidation of ethanol forms the two-electron product, acetaldehyde, and the four-electron product, acetic acid (AA), each of which can then undergo acid-catalyzed condensation reactions to form the secondary products 1,1′-diethoxyethane (DEE) and ethyl acetate (EA), respectively.[49,86−89] However, because the condensation reactions of the ethanol products are slow, electrolyses using previously prepared complexes of the type $Cp(PPh_3)Ru(\mu\text{-}Cl)(\mu\text{-}dppm)PtCl_2$ (**7**), $Cp(PPh_3)Ru(\mu\text{-}Cl)(\mu\text{-}dppm)PdCl_2$ (**8**), $Cp(PPh_3)RuCl(\mu\text{-}dppm)AuCl$ (**9**), $[\eta^5\text{-}C_5H_4CH_2CH_2NMe_2\cdot HCl]Ru(PPh_3)(\mu\text{-}I)(\mu\text{-}dppm)PdCl_2$ (**16**),[85] and $[\eta^5\text{-}C_5H_4CH_2CH_2NMe_2\cdot HCl]Ru(PPh_3)(\mu\text{-}I)(\mu\text{-}dppm)PtCl_2$ (**17**)[85] resulted in mixtures of products. Generally, if DCE is used as the solvent, the products observed are acetaldehyde and acetic acid; however, if the oxidation is performed in neat ethanol, both the initial and condensation products are observed.[90]

As reported for methanol, when 50 μL of ethanol was added to the cell, cyclic voltammograms of complexes **1**–**6** showed current increases at the redox potential corresponding to the oxidation of the second metal: M(II/IV) for M = Pt, Pd (see Figure 6 for the CV of complex **4**) or M(I/III) for M = Au.

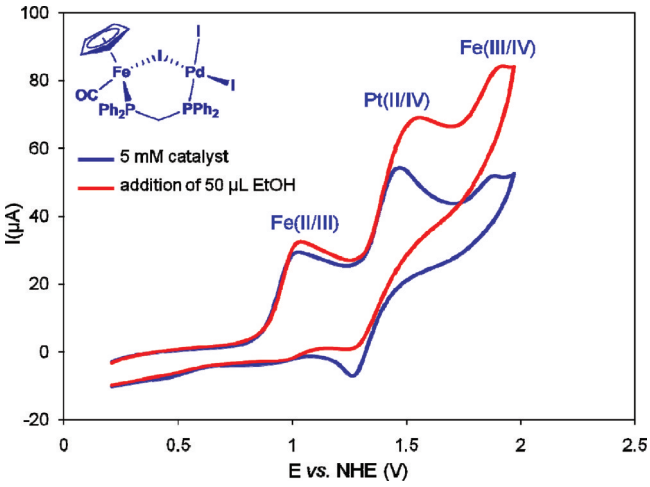

Figure 6. Cyclic voltammograms of complex **4**. Conditions: 0.1 M TBAT/DCE; 50 mV s^{-1} scan rate; glassy-carbon working electrode; Ag/Ag^+ reference electrode.

This rise in current is consistent with electrocatalytic oxidation of ethanol by complexes **1**–**6**. Bulk electrolysis was subsequently performed to identify the oxidation products.

Since complexes **1**–**6** are soluble in ethanol, electrolyses were performed in a solution of 0.1 M $TBABF_4$/EtOH at 1.7 V vs NHE (Table 3). The heterobimetallic Ru/Au and Fe/Au complexes **5** and **6** decomposed during the electrolysis, as previously observed during methanol oxidation. The Fe/Pd complex **4**, although stable during the experiment, yielded no oxidation products after bulk electrolysis. The Ru/Pt (**1**), Fe/Pt (**2**), and Ru/Pd (**3**) complexes all converted ethanol to the

dx.doi.org/10.1021/om101070z|*Organometallics* 2011, 30, 5568−5577

Table 3. Bulk Electrolysis Data for the Oxidation of Ethanol by Complexes 1−4

	amt of DEE in 4 mL (μmol)[a,b,c]			
charge (C)	Ru/Pt (**1**)	Fe/Pt (**2**)	Ru/Pd (**3**)	Fe/Pd (**4**)
20	30.4	15.1	59.1	n/o
40	62.1	35.8	95.8	n/o
60	105.1	54.5	134.0	n/o
80	150.9	78.2	171.0	n/o
100	175.7	110.5	193.5	n/o
150	197.6	168.3	249.0	n/o
200	237.5	181.4	312.9	n/o
		Ru/Pt (**1**)	Fe/Pt (**2**)	Ru/Pd (**3**)
CE[d] (%) after 200 C		22.9	17.5	30.2
TO[e] after 200 C		6	5	8

[a]Electrolyses were performed at 1.7 V vs NHE in pure ethanol. A 10 mM catalyst concentration was used for each experiment. [b]Determined by GC with respect to *n*-octane as an internal standard. n/o = no observable product. [c]No observable 4e product was detected during electrolysis. [d]CE denotes the ratio of charge needed to produce the observed yields of DEE vs the total charge passed during the experiment. [e]TO denotes the number of moles of DEE produced per mole of catalyst.

two-electron-oxidation product acetaldehyde, which was detected in the electrolyte solutions as its condensation product DEE. The primary two-electron-oxidation product acetaldehyde was not observed, nor was the four-electron-oxidation product AA or its ethanol condensate EA. In contrast to the results observed for neat methanol, the Fe/Pt complex **2** and the Ru/Pd complex **3** were more active in ethanol, resulting in 17.5% CE, TO = 5 and 30.2% CE, TO = 8, respectively, after 200 C of charge had been passed. The Ru/Pt complex **1** was less productive as an ethanol oxidation catalyst, having a CE of 22.9% and 8 TO compared to 63.1% and 12 TO in methanol. Due to the low current efficiencies, the catalysts were not examined under wet conditions.

CO_2 Evolution upon Electrooxidation of Methanol with Complexes 1−4. To detect gaseous products, a gas cell system for FTIR analysis of the headspace gases produced during the electrooxidation of methanol was fabricated. Since the FTIR spectrometer is outside the glovebox, the major difficulty is avoiding contamination by CO_2 from the atmosphere. Ambient CO_2 can be purged from the sample cell compartment by N_2 purge (Supporting Information, Figure S7), and a blank is always measured as a control before introducing the gas sample. All electrolyses were performed in the glovebox, and a gastight syringe was used to remove headspace gas samples during the process (every 20 C until 200 C of charge had been passed). For each sample, 60 mL of gas was introduced into the IR gas cell.

FTIR analysis of the headspace gas was performed for all methanol electrolyses with the heterobimetallic carbonyl compounds **1**−**4**, as well as **14** and **15**, and the mixtures of mononuclear model compounds. Among these experiments, heterobimetallic complexes **1** and **2** yielded sufficient quantities of CO_2 for FTIR detection and isotopic labeling experiments, while only traces of CO_2 were observed for the other compounds; thus, isotopic labeling studies were only performed for **1** and **2**. As observed in the FTIR spectra of headspace gases from bulk electrolysis of Ru/Pt complex **1** and Fe/Pt complex **2** (Figure 7), CO_2 could be detected (ν_{CO} 2361, 2338 cm^{-1}) along with traces of MF and a large quantity of methanol vapor

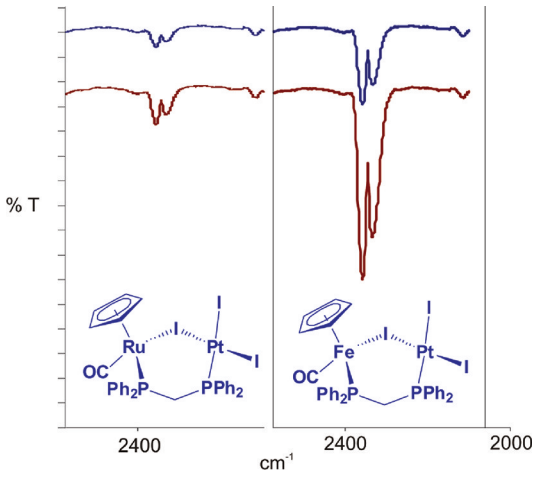

Figure 7. FTIR spectra (CO_2 region) of the headspace gases produced during the electrooxidation of methanol with the Ru/Pt complex **1** (left) and the Fe/Pt complex **2** (right) in the absence (blue line) and presence (red line) of water, after 200 C of charge had passed into the system.

(see the Supporting Information, Figures S8 and S9). For both compounds, electrolyses were performed in the presence and absence of water, which revealed that added water enhanced the formation of CO_2, as observed by the higher intensities of the CO_2 peak. Thus, with these results in hand, ^{13}C labeling experiments were carried out to confirm the origin of the CO_2 (from Ru−CO or Fe−CO vs from CH_3OH).

Isotopic Labeling Study. In order to determine the origin of the CO_2 formed during the electrolysis with complexes **1** and **2**, two experiments were performed: (i) using $^{12}CH_3OH$ and ^{13}CO-labeled Ru/Pt or Fe/Pt complex **1**-^{13}**CO** or **2**-^{13}**CO**, respectively, and (ii) using the unlabeled complexes **1** and **2** with $^{13}CH_3OH$. Bulk electrolyses were performed in the presence of a 1:1 mixture of $^{12}CH_3OH$ and $^{13}CH_3OH$ (about 2 mL of $^{13}CH_3OH$ was used for each experiment) for both (^{12}CO)-Ru/Pt complex **1** and (^{12}CO)-Fe/Pt complex **2**. If the ^{13}C-labeled CO_2 was formed by the electrooxidation of $^{13}CH_3OH$, it would be observed at the theoretical stretching frequency of 2296 cm^{-1}.[91,92] However, for both complexes **1** and **2**, no $^{13}CO_2$ could be detected, which indicated that the origin of CO_2 during the electrolysis was exclusively from the conversion of the CO ligand to CO_2 (Figure 8). This behavior is presumably the result of a competitive water-gas shift (WGS) reaction at the Ru−CO or Fe−CO moieties of **1** and **2**, respectively, and is suggested by the presence of added water, which favors the generation of CO_2. Such WGS reactions are well-known for metal carbonyl complexes such as those of Fe or Ru.[93,94] In order to confirm this hypothesis, the Fe/Pt complex **2**-^{13}**CO** was synthesized (vide supra) and the electrooxidation of methanol was carried out in the presence of added water. Bulk electrolysis results indicated that the concentration of $^{13}CO_2$ formed was significant, suggesting that the WGS reaction was responsible for cleavage of the CO ligand from the heterobimetallic Fe/Pt complex **2**. Indeed, only $^{13}CO_2$ could be observed in the FTIR spectrum when the labeled Fe/Pt complex **2**-^{13}**CO** was used for the electrolysis (Figure 8).

The ^{13}C-labeled Ru/Pt complex **1**-^{13}**CO** was synthesized and bulk electrolysis performed under similar conditions. FTIR data indicated the formation of trace amounts of $^{13}CO_2$, suggesting

dx.doi.org/10.1021/om101070z | *Organometallics* 2011, 30, 5568−5577

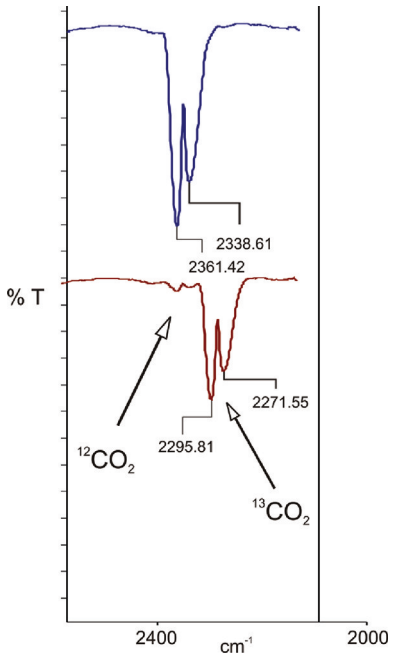

Figure 8. Isotopic labeling experiments: FTIR spectra (CO_2 region) of the headspace gases taken during the electrooxidation of methanol with heterobimetallic complexes **2** in presence of ^{13}C-methanol (blue line) and **2**-^{13}**CO** in the presence of ^{12}C-methanol (red line), both in the presence of added water.

that complex **1** also undergoes conversion of the ^{13}CO ligand to $^{13}CO_2$ by the WGS reaction during this process. However, this occurs to a lesser extent than is observed for the Fe/Pt complex **2**-^{13}**CO** (Supporting Information, Figure S10). The low concentration of CO_2 in the case of the Ru/Pt complex **1**-^{13}**CO** indicates higher stability toward CO loss, in comparison to the Fe/Pt system **2**-^{13}**CO**, as expected for a second-row transition metal.

Role of Water. During the electrooxidation of methanol under homogeneous conditions, water plays an important role as a product as well as a reactant in several steps of the electrolysis (Figure 9). Electrooxidation of methanol in the

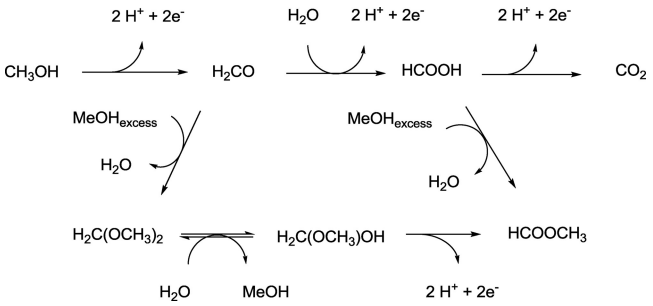

Figure 9. Electrooxidation of methanol.

presence of homogeneous catalysts results in the formation of formaldehyde and formic acid, which are the initial two- and four-electron-oxidation products formed during the process. In the presence of excess methanol these undergo fast condensation, leading to the formation of DMM, MF, and water[95−98] (Figure 9). Yields of the liquid products DMM and MF can be determined by GC analysis.[61,85] Previously, we have reported that electrochemical oxidation of DMM (0.16 M concentration) by **7** and **8** in DCE as solvent produces small amounts of MF.[61,62] This route is undoubtedly influenced by the water content, as the most probable pathway involves hydrolysis of DMM to the hemiacetal followed by oxidation to MF. Electrooxidation of DMM (50 μL, 0.57 M) using the Ru/Pd complex **3** in 0.1 M TBA(BF_4)/DCE also produced small amounts of MF; however, as described by Zhou and co-workers, this process is quite slow and requires acidic conditions to proceed.[99] When electrooxidation is performed in pure methanol, as in the case of these studies, this reaction is unlikely.

An additional effect of water is on the CO ligand of **1**−**3**. According to the IR experiments under dry and wet conditions, loss of CO involves attack by water to form CO_2 (the WGS reaction). For both **1** and **2**, higher concentrations of CO_2 were obtained when water was added (Figure 7, dry vs wet). In the case of the Ru/Pt complex **1**, CO loss is not occurring readily, as demonstrated by the low intensities of the CO_2 peaks. These results are consistent with water being involved in the decomposition of the complex, generating an inactive species which would be responsible for the lower CE and TO under wet conditions.

CONCLUSION

The catalytic activities for the electrooxidation of methanol and ethanol were investigated for a series of heterobimetallic carbonyl-containing Ru/Pt, Ru/Pd, and Ru/Au complexes as well as for their isoelectronic Fe/Pt, Fe/Pd, and Fe/Au analogues. The Ru/Pt, Ru/Pd, and Fe/Pd complexes **1**, **3**, and **4**, respectively, showed significant current enhancement in their cyclic voltammograms after addition of methanol or ethanol, consistent with electrooxidation of the alcohol. The small increases in current observed for the Ru/Au complex **5** and the Fe/Au complex **6** were most likely due to stoichiometric reactions of the complexes with methanol leading to decomposition.

The carbonyl-containing Ru/Pt and Ru/Pd complexes **1** and **3** are active catalysts for the electrochemical oxidation of methanol, showing good to moderate activity. The Fe/Pt complex **2** was the only Fe-containing heterobimetallic complex found to generate the electrooxidation products of methanol, DMM and MF, which were detected by GC analysis. In contrast, electrooxidation of methanol using the Fe/Pd, Ru/Au, and Fe/Au complexes **4**−**6**, respectively, produced no detectable oxidation products.

Electrocatalytic oxidation of ethanol using complexes **1**−**6** gave results similar to those observed for methanol. The Ru/Pt, Fe/Pt, and Ru/Pd complexes (**1**−**3**, respectively) were able to catalyze the electrooxidation of ethanol, while the Fe/Pd, Ru/Au, and Fe/Au complexes (**4**−**6**, respectively) showed no activity. Although neither the four-electron-oxidation product AA nor its condensation product EA was observed, complexes **1**−**3** were all able to produce DEE in good yield by two-electron oxidation followed by condensation.

FTIR analysis of the headspace gases produced during the electrochemical oxidation of methanol using Ru/Pt and Fe/Pt complexes **1** and **2** showed formation of CO_2, the theoretical six-electron oxidation product from methanol. However, isotopic labeling experiments using $^{13}CH_3OH$ revealed that CO_2 was not formed from the oxidation of methanol. The analogous experiment using the ^{13}CO-Fe/Pt complex **2**-^{13}**CO** with $^{12}CH_3OH$ resulted in formation of $^{13}CO_2$, which confirmed that the origin of the carbon dioxide was from

dx.doi.org/10.1021/om101070z|*Organometallics* 2011, 30, 5568−5577

oxidation of the carbonyl ligand. In the case of the ^{13}CO-Ru/Pt complex **1**-^{13}**CO**, $^{13}CO_2$ was observed only in trace amounts. This behavior is more pronounced in the presence of water and suggests that a WGS reaction may be involved during the formation of CO_2.

■ ASSOCIATED CONTENT

Supporting Information

Tables and figures giving carbonyl stretching frequencies for complexes **1** and **2** as well as the mononuclear compounds **11**, **13**, Cp(CO)Ru(κ^1-dppm)I, and Cp(CO)Fe(κ^1-dppm)I, cyclic voltammograms of complexes **3**−**5** with methanol as well as degradation of complex **5** with successive scans, product evolution for the electrooxidation of methanol using complexes **1**−**3** under wet and dry conditions, a schematic representation of the gas cell equipment used for FTIR detection of gaseous products, full FTIR spectra showing CO_2 evolution with complexes **2** and **3**, and isotopic labeling experiments with FTIR data of the headspace gases obtained from methanol electrooxidation. This material is available free of charge via the Internet at http://pubs.acs.org.

■ AUTHOR INFORMATION

Corresponding Author

*E-mail: lmwhite@chem.ufl.edu.

■ ACKNOWLEDGMENTS

We thank the NASA Glenn Research Center for partial support of this work under grant NAG 3-2930. M.C.C. thanks Prof. Jon D. Stewart for the loan of the J & W Scientific DB-5 GC column.

■ REFERENCES

(1) Adams, R. D., Cotton, F. A., Eds. *Catalysis by Di- and Polynuclear Metal Cluster Complexes*; Wiley-VCH: New York, 1998.
(2) Braunstein, P.; Rosé, J. In *Comprehensive Organometallic Chemistry II*; Abel, E. W.; Stone, F. G. A., Wilkinson, G., Eds.; Pergamon: Oxford, U.K., 1995; Vol. *10*, pp 351−380.
(3) Jones, N. D.; James, B. R. *Adv. Synth. Catal.* **2002**, *344*, 1126−1134.
(4) Süss-Fink, G.; Meister, G. *Adv. Organomet. Chem.* **1993**, *35*, 41−134.
(5) Wheatley, N.; Kalck, P. *Chem. Rev.* **1999**, *99*, 3379−3419.
(6) Xia, B. H.; Zhang, H. X.; Che, C. M.; Leung, K. H.; Phillips, D. L.; Zhu, N. Y.; Zhou, Z. Y. *J. Am. Chem. Soc.* **2003**, *125*, 10362−10374.
(7) Van Den Beuken, E. K.; Feringa, B. L. *Tetrahedron* **1998**, *54*, 12985−13011.
(8) Kuwabara, J.; Takeuchi, D.; Osakada, K. *Chem. Commun.* **2006**, 3815−3817.
(9) Yamaguchi, S.; Katoh, T.; Shinokubo, H.; Osuka, A. *J. Am. Chem. Soc.* **2007**, *129*, 6392−6393.
(10) Li, M.; Kowal, A.; Sasaki, K.; Marinkovic, N.; Su, D.; Korach, E.; Liu, P.; Adzic, R. R. *Electrochim. Acta* **2010**, *55*, 4331−4338.
(11) Anaya de Parrodi, C.; Walsh, P. J. *Angew. Chem., Int. Ed.* **2009**, *48*, 4679−4682.
(12) Adams, R. D.; Barnard, T. S. *Organometallics* **1998**, *17*, 2885−2890.
(13) Bosnich, B. *Inorg. Chem.* **1999**, *38*, 2554−2562.
(14) McCollum, D. G.; Bosnich, B. *Inorg. Chim. Acta* **1998**, *270*, 13−19.
(15) Stephan, D. W. *Coord. Chem. Rev.* **1989**, *95*, 41−107.
(16) Quebatte, L.; Scopelliti, R.; Severin, K. *Eur. J. Inorg. Chem.* **2006**, 231−236.
(17) McCleverty, J. A.; Ward, M. D. *Acc. Chem. Res.* **1998**, *31*, 842−851.
(18) Cornelissen, C.; Erker, G.; Kehr, G.; Fröhlich, R. *Organometallics* **2005**, *24*, 214−225.
(19) Velayudham, M.; Rajagopal, S. *Polyhedron* **2009**, *28*, 3043−3049.
(20) Santi, S.; Ceccon, A.; Bisello, A.; Durante, C.; Ganis, P.; Orian, L.; Benetollo, F.; Crociani, L. *Organometallics* **2005**, *24*, 4691−4694.
(21) Shibasaki, M.; Kanai, M.; Matsunaga, S.; Kumagai, N. *Acc. Chem. Res.* **2009**, *42*, 1117−1127.
(22) Jakob, A.; Ecorchard, P.; Rüffer, T.; Linseis, M.; Winter, R. F.; Lang, H. *J. Organomet. Chem.* **2009**, *694*, 3542−3547.
(23) Greenwood, B. P.; Forman, S. I.; Rowe, G. T.; Chen, C.-H.; Foxman, B. M.; Thomas, C. M. *Inorg. Chem.* **2009**, *48*, 6251−6260.
(24) Hamnett, A. In *Interfacial Electrochemistry. Theory, Experimental and Applications*; Wieckowski, A., Ed.; Marcel Dekker: New York, 1999.
(25) Hamnett, A. *Catal. Today* **1997**, *38*, 445−457.
(26) Enyo, M.; Machida, K.-i.; Fukuoka, A.; Ichikawa, M. In *Electrochemistry in Transition*; Murphy, O. J., Ed.; Plenum Press: New York, 1992; pp 359−369.
(27) Ross, P. N. *Electrochim. Acta* **1991**, *36*, 2053−2062.
(28) Zhao, H.; Li, L.; Yang, J.; Zhang, Y. *J. Power Sources* **2008**, *184*, 375−380.
(29) Zeng, J.; Lee, J. Y.; Zhou, W. *J. Power Sources* **2006**, *159*, 509−513.
(30) Iwasita, T. *Electrochim. Acta* **2002**, *47*, 3663−3674.
(31) Wang, H. S.; Wingender, C.; Baltruschat, H.; Lopez, M.; Reetz, M. T. *J. Electroanal. Chem.* **2001**, *509*, 163−169.
(32) Gasteiger, H. A.; Markovic, N.; Ross, P. N.; Cairns, E. J. *J. Electrochem. Soc.* **1994**, *141*, 1795−1803.
(33) Kabbabi, A.; Faure, R.; Durand, R.; Beden, B.; Hahn, F.; Leger, J. M.; Lamy, C. *J. Electroanal. Chem.* **1998**, *444*, 41−53.
(34) Morimoto, Y.; Yeager, E. B. *J. Electroanal. Chem.* **1998**, *444*, 95−100.
(35) Watanabe, M.; Uchida, M.; Motoo, S. *J. Electroanal. Chem. Interfacial Electrochem.* **1987**, *229*, 395−406.
(36) Roth, C.; Martz, N.; Hahn, F.; Leger, J.-M.; Lamy, C.; Fuess, H. *J. Electrochem. Soc.* **2002**, *149*, E433−E439.
(37) Leger, J. M.; Lamy, C. *Ber. Bunsen-Ges. Phys. Chem.* **1990**, *94*, 1021−1025.
(38) Neburchilov, V.; Wang, H.; Zhang, J. *Electrochem. Commun.* **2007**, *9*, 1788−1792.
(39) Papadimitriou, S.; Armyanov, S.; Valova, E.; Hubin, A.; Steenhaut, O.; Pavlidou, E.; Kokkinidis, G.; Sotiropoulos, S. *J. Phys. Chem. C* **2010**, *114*, 5217−5223.
(40) Alyousef, Y. M.; Datta, M. K.; Yao, S. C.; Kumta, P. N. *J. Phys. Chem. Solids* **2009**, *70*, 1019−1023.
(41) Spinacé, E. V.; Neto, A. O.; Linardi, M. *J. Power Sources* **2004**, *129*, 121−126.
(42) Lee, K.-S.; Park, I.-S.; Park, H.-Y.; Jeon, T.-Y.; Cho, Y.-H.; Sung, Y.-E. *J. Electrochem. Soc.* **2009**, *156*, B1150−B1155.
(43) Wu, B.; Hu, D.; Kuang, Y.; Liu, B.; Zhang, X.; Chen, J. *Angew. Chem., Int. Ed.* **2009**, *48*, 4751−4754.
(44) Wang, R.; Li, H.; Feng, H.; Wang, H.; Lei, Z. *J. Power Sources* **2010**, *195*, 1099−1102.
(45) Asthagiri, A.; Sholl, D. S. *Surf. Sci.* **2005**, *581*, 66−87.
(46) Leger, J. M. *J. Appl. Electrochem.* **2001**, *31*, 767−771.
(47) Beden, B.; Lamy, C.; Bewick, A.; Kunimatsu, K. *J. Electroanal. Chem. Interfacial Electrochem.* **1981**, *121*, 343−347.
(48) Zhou, C.; Wang, H.; Peng, F.; Liang, J.; Yu, H.; Yang, J. *Langmuir* **2009**, *25*, 7711−7717.
(49) Kadirgan, F.; Beyhan, S.; Atilan, T. *Int. J. Hydrogen Energy* **2009**, *34*, 4312−4320.
(50) Hamnett, A.; Kennedy, B. J. *Electrochim. Acta* **1988**, *33*, 1613−1618.
(51) Kardash, D.; Korzeniewski, C.; Markovic, N. *J. Electroanal. Chem.* **2001**, *500*, 518−523.
(52) Kawaguchi, T.; Sugimoto, W.; Murakami, Y.; Takasu, Y. *J. Catal.* **2005**, *229*, 176−184.

(53) Sieben, J. M.; Duarte, M. M. E.; Mayer, C. E. *ChemCatChem* **2009**, *2*, 182−189.
(54) Shivhare, M. R.; Jackson, C. L.; Scott, K.; Martin, E. B. *J. Power Sources* **2007**, *173*, 240−248.
(55) MacDonald, J. P.; Gualtieri, B.; Runga, N.; Teliz, E.; Zinola, C. F. *Int. J. Hydrogen Energy* **2008**, *33*, 7048−7061.
(56) Watanabe, M.; Motoo, S. *J. Electroanal. Chem. Interfacial Electrochem.* **1975**, *60*, 267−273.
(57) Watanabe, M.; Motoo, S. *J. Electroanal. Chem. Interfacial Electrochem.* **1975**, *60*, 276−283.
(58) Ávila-García, I.; Ramírez, C.; Hallen López, J. M.; Arce Estrada, E. M. *J. Alloys Compd.* **2010**, *495*, 462−465.
(59) Tess, M. E.; Hill, P. L.; Torraca, K. E.; Kerr, M. E.; Abboud, K. A.; McElwee-White, L. *Inorg. Chem.* **2000**, *39*, 3942−3944.
(60) Matare, G.; Tess, M. E.; Abboud, K. A.; Yang, Y.; McElwee-White, L. *Organometallics* **2002**, *21*, 711−716.
(61) Yang, Y.; McElwee-White, L. *Dalton Trans.* **2004**, 2352−2356.
(62) Anthony, C. R.; McElwee-White, L. *J. Mol. Catal. A: Chem.* **2005**, *227*, 113−117.
(63) Bolm, C.; Legros, J.; Le Paih, J.; Zani, L. *Chem. Rev.* **2004**, *104*, 6217−6254.
(64) Plietker, B., Ed. *Iron Catalysis in Organic Chemistry Reactions and Applications*; Wiley-VCH: Weinheim, Germany, 2008.
(65) Enthaler, S.; Junge, K.; Beller, M. *Angew. Chem., Int. Ed.* **2008**, *47*, 3317−3321.
(66) Correa, A.; Garcia, M. O.; Bolm, C. *Chem. Soc. Rev.* **2008**, *37*, 1108−1117.
(67) Sherry, B. D.; Fürstner, A. *Acc. Chem. Res.* **2008**, *41*, 1500−1511.
(68) Sarhan, A. A. O.; Bolm, C. *Chem. Soc. Rev.* **2009**, *38*, 2730−2744.
(69) Qin, C.; Jiao, N. *J. Am. Chem. Soc.* **2010**, *132*, 15893−15895.
(70) Serra, D.; Abboud, K. A.; Hilliard, C. R.; McElwee-White, L. *Organometallics* **2007**, *26*, 3085−3095.
(71) Haines, R. J.; DuPreez, A. L. *J. Chem. Soc., Dalton Trans.* **1972**, 944−948.
(72) Brown, D. A.; Lyons, H. J.; Sane, R. T. *Inorg. Chim. Acta* **1970**, *4*, 621−625.
(73) Coville, N. J.; Darling, E. A. *J. Organomet. Chem.* **1984**, *277*, 105−111.
(74) Coville, N. J.; Darling, E. A.; Hearn, A. W.; Johnston, P. *J. Organomet. Chem.* **1987**, *328*, 375−385.
(75) Haines, R. J.; DuPreez, A. L. *Inorg. Chem.* **1972**, *11*, 330−336.
(76) Nagashima, H.; Mukai, K.; Shiota, Y.; Yamaguchi, K.; Ara, K.; Fukahori, T.; Suzuki, H.; Akita, M.; Morooka, Y.; Itoh, K. *Organometallics* **1990**, *9*, 799−807.
(77) Dev, S.; Selegue, J. P. *J. Organomet. Chem.* **1994**, *469*, 107−110.
(78) Blackmore, T.; Cotton, J. D.; Bruce, M. I.; Stone, F. G. A. *J. Chem. Soc. A* **1968**, 2931−2936.
(79) Manning, A. R. *J. Chem. Soc. A* **1968**, *6*, 1319−1324.
(80) Haines, R. J.; Du Preez, A. L. *J. Chem. Soc. A* **1970**, *13*, 2341−2346.
(81) Dooling, D.; Joorst, G.; Mapolie, S. F. *Polyhedron* **2001**, *20*, 467−476.
(82) Hsu, M.-A.; Yeh, W.-Y.; Chiang, M. Y. *J. Organomet. Chem.* **1998**, *552*, 135−143.
(83) Orth, S. D.; Terry, M. R.; Abboud, K. A.; Dodson, B.; McElwee-White, L. *Inorg. Chem.* **1996**, *35*, 916−922.
(84) Yang, Y.; Abboud, K. A.; McElwee-White, L. *Dalton Trans.* **2003**, 4288−4296.
(85) Serra, D.; McElwee-White, L. *Inorg. Chim. Acta* **2008**, *361*, 3237−3246.
(86) Lamy, C.; Belgsir, E. M.; Leger, J. M. *J. Appl. Electrochem.* **2001**, *31*, 799−809.
(87) Leger, J. M.; Rousseau, S.; Coutanceau, C.; Hahn, F.; Lamy, C. *Electrochim. Acta* **2005**, *50*, 5118−5125.
(88) Vigier, F.; Rousseau, S.; Coutanceau, C.; Leger, J. M.; Lamy, C. *Top. Catal.* **2006**, *40*, 111−121.
(89) Rousseau, S.; Coutanceau, C.; Lamy, C.; Leger, J. M. *J. Power Sources* **2006**, *158*, 18−24.
(90) Correia, M. C.; Moghieb, A.; Goforth, S. K.; McElwee-White, L. *ECS Trans.* **2009**, *19*, 13−21.
(91) Basset, J. M.; Candy, J. P.; Choplin, A.; Nedez, C.; Quignard, F.; Santini, C. C.; Theolier, A. *Mater. Chem. Phys.* **1991**, *29*, 5−32.
(92) Silverstein, R. M.; Webster, F. X.; Kiemle, D. In *Spectrometric Identification of Organic Compounds*, 7th ed.; Wiley-VCH: Weinheim, Germany, 2005; pp 72−108.
(93) Ford, P. C. *Acc. Chem. Res.* **1981**, *14*, 31−37.
(94) King, R. B. *J. Organomet. Chem.* **1999**, *586*, 2−17.
(95) Yamanaka, I.; Otsuka, K. *Electrochim. Acta* **1989**, *34*, 211−214.
(96) Nakajima, H.; Kita, H. *Electrochim. Acta* **1988**, *33*, 521−526.
(97) Lin, W. F.; Wang, J. T.; Savinell, R. F. *J. Electrochem. Soc.* **1997**, *144*, 1917−1922.
(98) Iwasita, T.; Vielstich, W. *J. Electroanal. Chem. Interfacial Electrochem.* **1986**, *201*, 403−408.
(99) Zhou, Z.-Y.; Chen, D.-J.; Li, H.; Wang, Q.; Sun, S.-G. *J. Phys. Chem. C* **2008**, *112*, 19012−19017.